
Stress Magnitudes in the Crust: Constraints from Stress Orientation and Relative Magnitude Data

Mary Lou Zoback and Marian Magee

Phil. Trans. R. Soc. Lond. A 1991 **337**, 181-194

doi: 10.1098/rsta.1991.0115

Email alerting service

Receive free email alerts when new articles cite this article - sign up in the box at the top right-hand corner of the article or click [here](#)

To subscribe to *Phil. Trans. R. Soc. Lond. A* go to:

<http://rsta.royalsocietypublishing.org/subscriptions>

Stress magnitudes in the crust: constraints from stress orientation and relative magnitude data

BY MARY LOU ZOBACK¹† AND MARIAN MAGEE²

¹*Geophysikalisches Institut, Universität Karlsruhe, Hertzstrasse 16, 7500 Karlsruhe 21, F.R.G.*

²*U.S. Geological Survey, MS 977, 345 Middlefield Road, Menlo Park, California 94025, U.S.A.; Department of Geophysics, Stanford University, Stanford, California 94305, U.S.A.*

The World Stress Map Project is a global cooperative effort to compile and interpret data on the orientation and relative magnitudes of the contemporary *in situ* tectonic stress field in the Earth's lithosphere. Horizontal stress orientations show regionally uniform patterns throughout many continental intraplate regions. These regional intraplate stress fields are consistent over regions 1000–5000 km wide or *ca.* 100 times the thickness of the upper brittle part of the lithosphere (*ca.* 20 km) and about 10–15 times the thickness of typical continental lithosphere (*ca.* 150–200 km).

Relative stress magnitudes or stress régimes in the lithosphere are inferred from direct *in situ* stress measurements and from the style of active faulting. The intraplate stress field in both the oceans and continents is largely compressional with one or both of the horizontal stresses greater than the vertical stress. The regionally uniform horizontal intraplate stress orientations are generally consistent with either relative or absolute plate motions indicating that plate-boundary forces dominate the stress distribution within the plates. Since most regions of normal faulting occur in areas of high elevation, the extensional stress régimes in these areas can be attributed to superimposed bouyancy forces related to crustal thickening and/or lithosphere thinning; stresses derived from these bouyancy forces locally exceed mid-plate compressional stresses.

Evaluating the effect of viscous drag forces acting on the plates is difficult. Simple driving or resisting drag models (with shear tractions acting parallel or antiparallel to plate motion) are consistent with stress orientation data; however, the large lateral stress gradients across broad plates required to balance these tractions are not observed in the relative stress magnitude data. Current models of stresses due to whole mantle flow inferred from seismic tomography models (and with the inclusion of the effect of high density slabs) predict a general compressional stress state within continents but do not match the broad-scale horizontal stress orientations. The broad regionally uniform intraplate stress orientations are best correlated with compressional plate-boundary forces and the geometry of the plate boundaries.

1. Introduction

A global compilation of *in situ* stress data is currently underway as part of the World Stress Map (WSM) project, a Task Group of the International Lithosphere Program.

† Permanent address: U.S. Geological Survey, MS 977, 345 Middlefield Road, Menlo Park, California 94025, U.S.A.

Phil. Trans. R. Soc. Lond. A (1991) **337**, 181–194

Printed in Great Britain

181

The goal of this project is to compile and interpret data on the intraplate tectonic stress field. More than 5700 data points on stress orientation and relative magnitudes (and absolute stress magnitudes where available) in the upper crust have been compiled to date. The focus of the WSM effort is to define the stress field within the plates and within broad deformational zones adjacent to plate boundaries; data on the stress state along plate boundaries (e.g. mid-ocean ridges or along or within Benioff zones) have not in general been compiled as the kinematics of these boundaries are generally well known. Through interpretation of the intraplate stress data, constraints can be placed on the magnitudes of both broad scale and local sources of stress acting on the lithosphere.

Results to date of the WSM project will be summarized in a special issue of *J. geophys. Res.*, now nearly completed. The special issue contains over 20 papers covering all aspects of the project from description of the data, discussion of regional stress patterns and their relationship to tectonics, as well as finite element modelling of the stress data to constrain the magnitudes of forces acting on the plates.

The purpose of this paper is to investigate a specific aspect of stress in the lithosphere, the implications of the global stress database for the magnitude of stress in the upper lithosphere. Relative stress magnitudes are inferred from the style of faulting observed in over 3032 intraplate focal mechanisms compiled worldwide, allowing a characterization of mean stress levels within the plates relative to the lithostat.

Following early finite element modelling of global intraplate stress patterns by Richardson *et al.* (1979), numerous modelling papers have demonstrated that most of the broad-scale stress patterns observed within the interiors or plates can be attributed directly to the effects of plate boundary forces (see summary of recent modelling attempts in Zoback (1991*a*)). Drag forces typically are assumed to be resistive and of small magnitude and used to balance the torque on individual plates (Richardson *et al.* 1979; Cloetingh & Wortel 1986; Richardson & Reding 1991). Recently Bai *et al.* (1991) have calculated the stress effect in the lithosphere of drag related to flow induced by deep mass inhomogeneities in the mantle inferred from global seismic tomography models. The possible influence on the intraplate stress field of this drag, which is related to large-scale mantle flow, is evaluated by a comparison between the WSM observations and the stress patterns (both orientation and relative magnitude) predicted by Bai *et al.* (1991).

2. First-order patterns of stress in the lithosphere

The available global stress orientation data are shown in figure 1, which plots the maximum horizontal stress ($S_{H,max}$) orientation. In areas of extensional stress $S_{H,max}$ corresponds to the intermediate stress S_2 ; in all other regions $S_{H,max}$ corresponds to the maximum stress, S_1 . The data are derived from a variety of geologic and geophysical indicators: the *P*- and *T*-axes of earthquake focal mechanisms, well-bore breakouts, *in situ* stress measurements by hydraulic fracturing and overcoring, volcanic vent alignments, and fault slip data. The geologic data included are generally of Quaternary age (or in regions of possible multiple Quaternary deformation episodes, the data correspond to the youngest deformation). In some stable areas (such as the eastern United States) fault slip data as old as post-Miocene have been included. Note that the lengths of the oriented lines shown on figure 1 correspond to quality or reliability of the data as a tectonic stress indicator. This

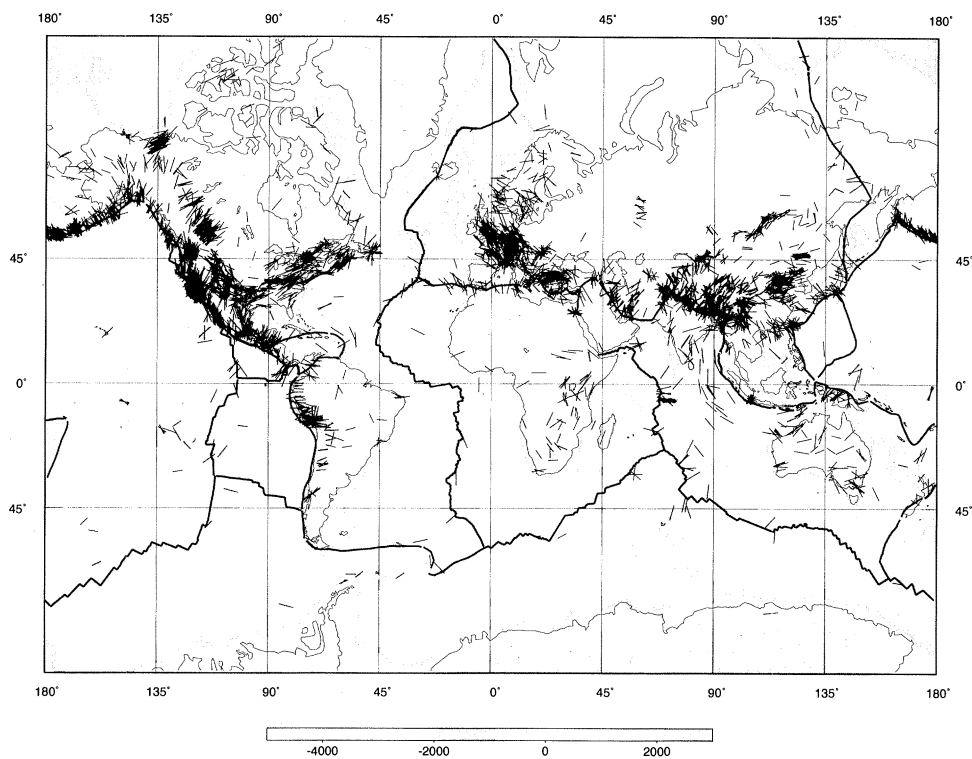


Figure 1. World Stress Map, Mercator projection. $S_{H,max}$ orientations are plotted, length of lines are proportional to quality.

quality ranking system is based on accuracy of the data, the depth interval sampled and the general reliability of the technique used. A detailed description of the theory and limitations of these various stress indicators and the quality ranking system has been given in several recent papers (Zoback & Zoback 1989, 1991; Zoback 1991*a*), the reader is referred to these papers for additional information. A large size colour map of the data shown here in figure 1 is included in Zoback (1991*a*).

Figure 2 is a generalized stress map derived from mean stress orientations for regions of dense data coverage. Absolute velocity trajectories for individual plates computed using absolute velocity poles AM1-2 of Minster & Jordan (1978) are also given. Many of the general conclusions of the global data compilation based on stress orientations (Zoback *et al.* 1989; Zoback 1991*a*) can be verified by inspection of figures 1 and 2.

1. Stress orientations inferred from different techniques yield consistent and similar orientations despite the different depths and volumes of rock sampled, the data indicate that both the orientation and relative magnitude of the stress field are generally uniform in depth through brittle layer.

2. The different stress indicators define a tectonic stress field and indicate that broad regions of the Earth's crust (1000s km on a side) are subject to uniform patterns of stress orientation, despite geologic and structural complexity of the upper crust, the source of these regionally uniform stress fields must be broad scale.

3. There is a correlation between $S_{H,max}$ orientations and the directions of absolute plate motion for broad regions of many plates.

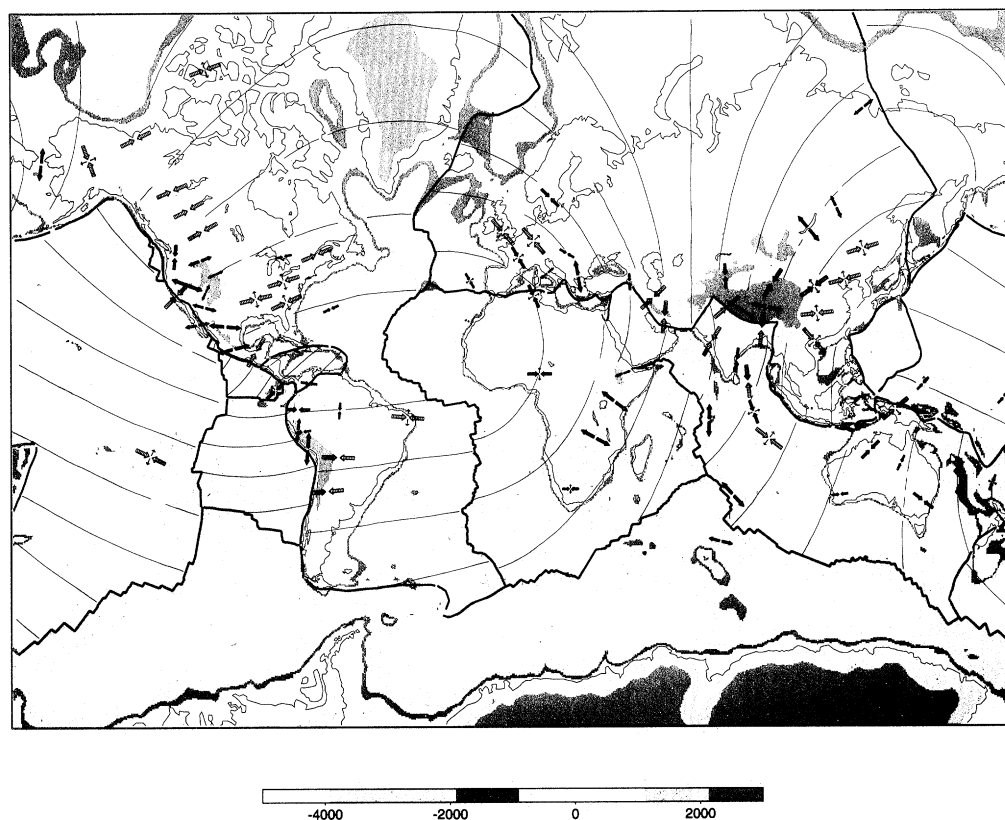


Figure 2. Generalized stress map of the world. Large arrows indicate mean stress directions for dense clusters of data. Inward pointing arrows indicate $S_{H,max}$ orientations for compressive stress regimes where $S_{H,max}$ coincides with S_1 and one or both of the horizontal stresses exceeds the vertical stress. Outward pointing arrows show $S_{H,min}$ orientations. Thick outward pointing arrows indicate regions of extensional stress régime where both horizontal stresses are less than the vertical stress. Thin outward pointing arrows plotted together with inward pointing arrows indicate a strike-slip faulting stress régime. Coverage is non-uniform due to the non-uniform data coverage in figure 1. Light lines are absolute velocity trajectories from model AM1-2 of Minster & Jordan (1978).

Finite-element modelling to predict intraplate stresses from both body forces and tractions acting on the plates has now been completed for a number of individual plates. The consistent ENE $S_{H,max}$ direction in the eastern United States and throughout much of Canada is generally parallel to the direction of absolute motion of North America (Zoback *et al.* 1986); however, Richardson & Reding (1991) demonstrate that this direction is also consistent with ridge push forces. Similarly, $S_{H,max}$ orientations in South America agree both with ridge push and absolute motion directions (Assumpcao 1991). Meijer & Wortel (1991) and Jurdy & Stefanick (1991) both conclude that ridge push is the dominant force responsible for the E-W compression in South America, with local influence of trench suction or buoyancy forces causing extension in the Andean region. Meijer & Wortel (1991) also concluded that driving drag could not be ruled-out as an important force affecting South America; they did not, however, compute the predicted stresses for a driving drag model.

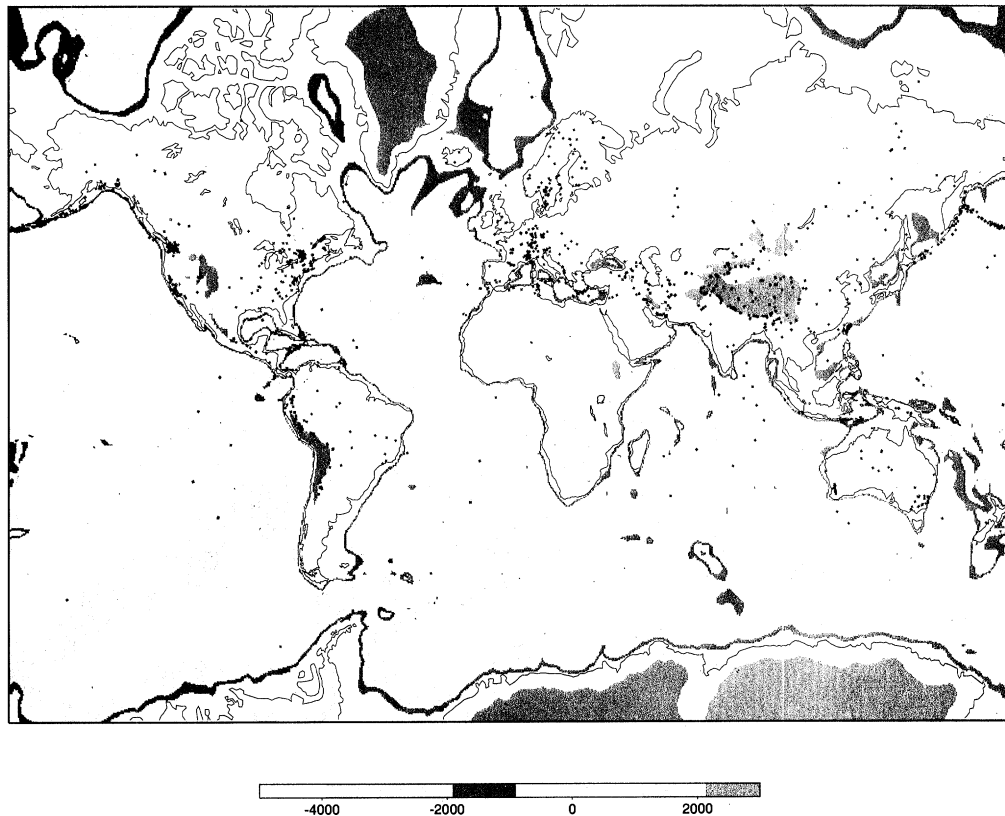


Figure 3. Location (by small crosses) of all data indicating a thrust faulting stress régime ($S_{H,max} > S_{H,min} > S_V$) in the WSM database.

$S_{H,max}$ orientations are subparallel to absolute plate motion in western Europe where the absolute plate velocity is poorly resolved; however, an even better correlation is observed between $S_{H,max}$ orientations and the relative velocity trajectories for the convergence of Africa and Eurasia (Müller *et al.* 1991). The NNW to NW compression throughout western Europe (excluding the Mediterranean region) has been successfully modelled as the combined effect of ridge push along the northwestern border of the plate and convergence and continental convergence and collision between Africa and Eurasia along the southern border (Grunthal & Stromeyer 1991).

Sparse stress data from western and southernmost Africa indicate E–W compression consistent with ridge-push directions and nearly orthogonal to the absolute motion direction (Zoback 1991*a*). However, in eastern Africa, the intraplate stress field is dominated by extensional stresses related to buoyancy forces derived from a thin lithosphere and warm upwelling upper mantle (see §3*a*).

The stress pattern in Australia is complex; however, the best data in central Australia suggest NNE to NE compression approximately in the direction of absolute motion, but also consistent with ridge push along the southern boundary of the plate and arc collision along the northern boundary. E–W compression is well documented in both southeastern and southwestern Australia and is difficult to explain in terms of plate boundary forces.

In other places, $S_{H,max}$ directions do not correlate directly with absolute or relative plate motion but are clearly related to plate-boundary forces. For example, the radial pattern of $S_{H,max}$ orientations in eastern Eurasia fanning out from the Himalayan collision have been successfully modelled by a number of workers as the result of collisional forces related to the indenter geometry of India into Eurasia (a recent example of such modelling is given in England & Houseman (1989)). Thus once again the influence of forces acting along the plate boundary (in this case related to the Eindentor of India into Eurasia (Molnar & Tapponier 1975)) is seen to be the dominant force influencing the stress field 1000s of km from the plate boundary.

Clearly plate driving forces play a critical role in determining the stress field in the interior of the plates. However, the geometry of the plate boundary apparently plays an equally important role in determining the actual orientation of the intraplate stress field. Two compressive forces, continental collision and ridge push (particularly for plates with no or only a very small attached slab), play a dominant role in determining the intraplate stress field as first noted by Richardson *et al.* (1979). Net slab forces (balance of slab pull and both viscous and frictional resistance to subduction) are probably generally small and compressive (Richardson *et al.* 1979; Cloetingh & Wortel 1986) as demonstrated by an absence of extensional intraplate earthquakes in old oceanic crust (Wiens & Stein 1985). The role of drag forces is more difficult to evaluate since, as Richardson (1991) points out, the ridge push and absolute motion torque poles are nearly identical for most plates; thus effects of the ridge push and either driving drag or resisting drag in the direction of absolute plate motion can not be differentiated on the basis of stress orientations alone. However, there are considerable differences in the predicted stress magnitudes for drag versus ridge-push forces. Stress magnitudes due to ridge push are compressive constant throughout the continents and in old oceans (where oceanic topography no longer follows the t^{-2} cooling curve); however, tractions across the base of the plate due to drag induce stress gradients across the plates. Thus to properly evaluate drag we need information on stress magnitudes.

3. Magnitude of stress in the lithosphere

The World Stress Map project has systematically compiled data on stress orientations; however, since the stress field is a tensor, complete characterization requires magnitude information. Available stress magnitude determinations (from *in situ* stress measurements) have also been compiled; however, these data represent only about 2% (103/5701) of the database (and generally sample only the upper 1–2 km of the Earth's crust). Because both technical and economic constraints limit the depth of stress magnitude measurements to generally less than seismogenic depths (5–20 km), we must infer absolute stress magnitudes either from laboratory studies, or from downward extrapolation of near-surface stress measurements.

However, information on relative or absolute stress magnitudes obtained from earthquake focal mechanisms, *in situ* stress measurements, and young fault slip data can be used to categorize the data into three main stress régimes: normal faulting, strike-slip faulting, and thrust faulting (as defined below). In figures 3–5 the location of data corresponding to each of these three régimes is indicated by small crosses.

For data where information on the plunges of either the P -, B - and T -axes or S_1 , S_2 , and S_3 axes are available, specific ranges of plunges were used to categorize the data into the three stress régimes. The rationale for these specific ranges of plunges

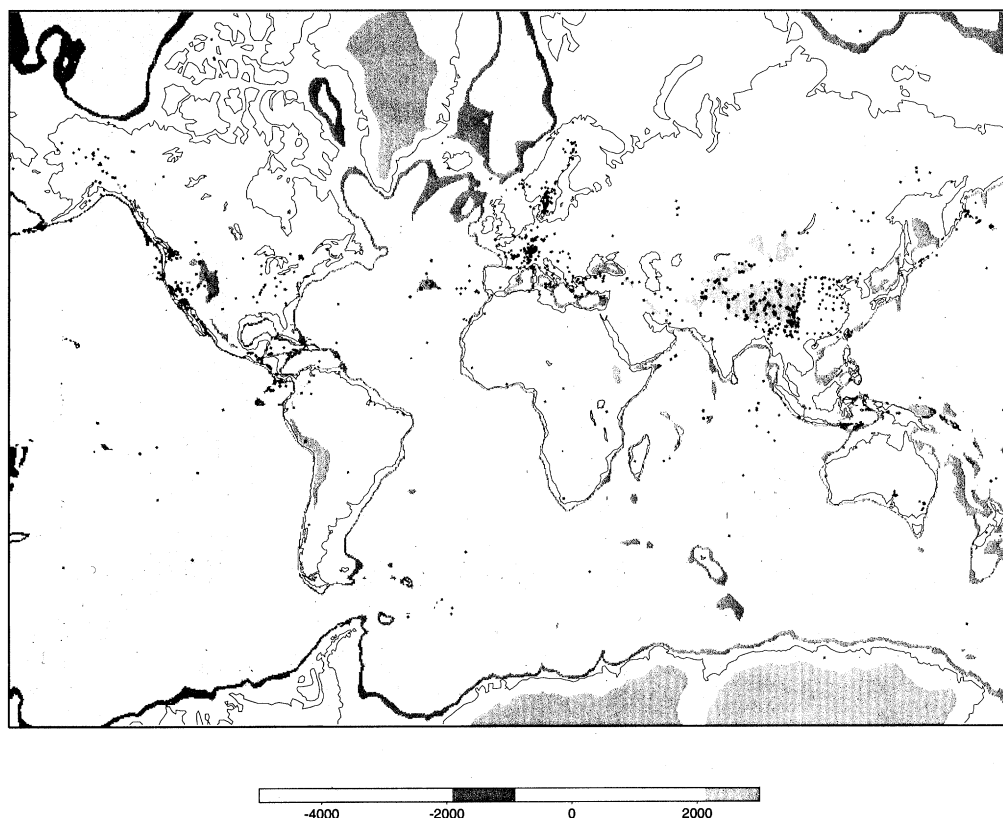


Figure 4. Location (by small crosses) of all data indicating a strike-slip faulting stress régime ($S_{H,max} > S_V > S_{H,min}$) in the WSM database.

is based on an assumption of principal stresses in the crust lying in approximately horizontal and vertical planes, the actual values somewhat subjective (see discussion in Zoback 1991 *a*). The three main stress régimes and style of faulting (and associate ranges of axes' plunges) are:

- | | P/S_1 plunge | B/S_2 plunge | T/S_3 plunge |
|--|------------------------------|-------------------|------------------------------|
| (1) extensional stress régime ($S_V > S_{H,max} > S_{H,min}$), normal dip slip (figure 5) | $pl > 52^\circ$, | | $pl < 35^\circ$, |
| or | $40^\circ < pl < 52^\circ$, | | $pl < 20^\circ$; |
| (2) strike-slip stress régime ($S_{H,max} > S_V > S_{H,min}$), dominantly horizontal slip (figure 4) | $pl < 40^\circ$, | $pl > 45^\circ$, | $pl < 20^\circ$, |
| or | $pl < 20^\circ$, | $pl > 45^\circ$, | $pl < 40^\circ$, |
| (3) thrust stress régime ($S_{H,max} > S_{H,min} > S_V$), reverse dip slip (figure 3) | $pl < 20^\circ$, | | $40^\circ < pl < 52^\circ$, |
| or | $pl < 35^\circ$, | | $pl > 52^\circ$. |

Another general conclusion of the WSM project is clear when comparing figures 3–5: most midplate regions are characterized by compressional deformation (strike-slip and thrust faulting stress régimes), regions of extensional stress régime occur primarily in topographically high areas in both the continents and the oceans.

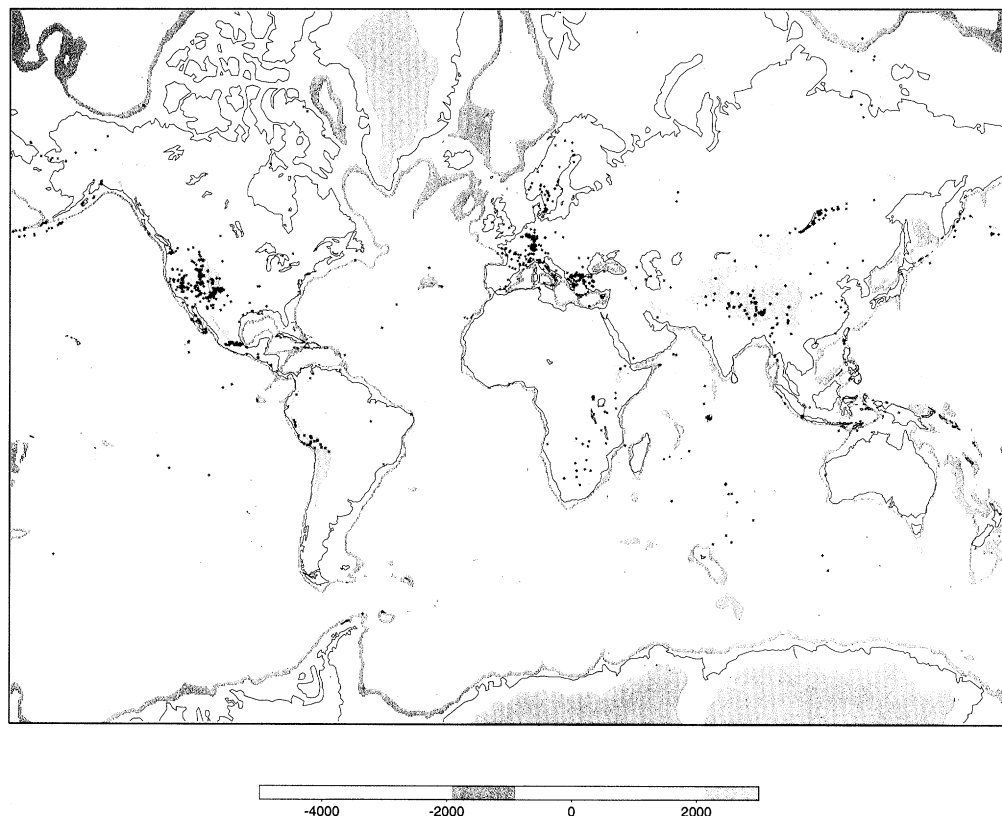


Figure 5. Location (by small crosses) of all data indicating a normal faulting stress régime ($S_V > S_{H,max} > S_{H,min}$) in the WSM database.

In detail, a number of conclusions can be drawn about relative stress magnitudes in the lithosphere by comparing the distribution of data shown on figures 3–5. As can be seen in figure 3, much of the Australian continent is dominated by thrust régime. Similarly thrust faulting dominates in southeastern Canada (possibly a local effect related in part to glacial rebound influence (Zoback 1991*b*)), throughout continental South America, and in a broad zone of continental convergence in the Caucasus. Dominantly strike–slip deformation (figure 4) is seen along the San Andreas system, western Africa, and eastern China, and in continental Alaska. Comparison of figures 3 and 4 indicate that many other midplate areas are subject to a combination of strike–slip and thrust faulting régimes: much of the central and eastern United States, the Pacific Northwest of the United States (region overlying the subducted Juan de Fuca plate), old parts of the Pacific plate, the eastern Indian ocean and India subcontinent, Fennoscandia, western Europe, and the Tibetan Plateau. As discussed below, these last two areas also contain a fair amount of normal faulting data but as can be seen in figure 1 the $S_{h,max}$ orientations are constant for data in all three régimes.

The normal faulting stress data mostly occur in elevated regions: western U.S. Cordillera, the High Andes, East African rift, Tibetan plateau, Baikal rift, and the western Indian Ocean. Other areas of extension occur in topographically low regions, most notably the Aegean region which lies in a back-arc setting. There are also a

large number of normal faulting earthquakes in western Europe, well north of the Alps. This is in marked contrast to midplate North America where normal faulting is quite rare.

In some cases the source of the high elevation in some of the extensional regions may be simply related to thickened crust (Andes and the Tibetan Plateau); however, in both these regions the elevation has been attributed to combined effects of a thickened crust and a thinned mantle lithosphere (see Isacks (1988) for discussion of upper mantle structure beneath the Andean region and England & Houseman (1989) for a discussion of the upper mantle contribution to explain both rapid uplift and the extensional state of stress on the Tibetan plateau). In many other regions (such as the western U.S., East Africa, and Baikal rift, the crust is quite thin (30–35 km thick) and the source of the high elevation is clearly related to a thinned mantle lithosphere and upwelling hot asthenosphere (Thompson & Zoback (1979) for western U.S., Henry *et al.* (1990) for the East African rift, and Zorin & Rogozhina (1978) for the Baikal rift). Thus the state of stress in many extensional regions can be related to the local effects of buoyancy forces derived not only from a crustal root, but in many cases dominated by the effects of thermal upwelling and thinned lithosphere (as described below).

(a) *Role of buoyancy forces*

It is clear from the general pattern of midplate compression that areas of extension require additional superimposed forces to produce the normal faulting stress régime in which both horizontal stresses are least than the vertical stress. In fact as can be seen in figure 5, the direction of extension in many of the extensional regions is generally perpendicular to the trend of the topographic bulge indicating the importance of the buoyancy force in overcoming the regional midplate compressional stress state. This observation can be used to place limits on the average magnitude of the mid-plate compression in the uppermost lithosphere due to plate driving forces such as ridge push and continental collision (Artyushkov 1973; Fleitout & Froidevaux 1982, 1983).

The horizontal compression of the ridge-push force is a result of the horizontal density contrast associated with the cooling and thickening of the oceanic lithosphere with age. Because the ocean floor topography and densities are generally well known, the ridge-push force is the easiest force to quantify and estimates of the total force range from $2\text{--}3 \times 10^{12} \text{ N m}^{-1}$ (Frank 1972; Lister 1975; Parsons & Richter 1980), equivalent to *ca.* 20–30 MPa of stress averaged over a 100 km thick lithosphere. The actual magnitude of stress induced in the uppermost lithosphere depends upon how this force is distributed; the ductile nature of the lower part of the lithosphere causes a redistribution of any stress applied to the whole lithosphere and results in a stress amplification in the upper, more brittle part of the lithosphere (Kusznir & Bott 1977). For realistic rheologies, Kusznir & Park (1984, 1987) estimate a stress amplification by a factor of about 2–3 in the uppermost continental lithosphere for an applied compressional stress with surface heat flow of 60 mW m^{-2} .

Estimating stresses related to lateral density contrasts in regions of elevated topography is critically dependent on the assumptions about the density distribution within the lithosphere (England & Houseman 1989). However, lateral variations in this buoyancy-related stress are directly related to variations in geoid height; Froidevaux & Isacks (1984) use the geoid anomaly associated with the 4000 m high Altiplano-Puna plateau of the Andes to compute a buoyancy related force of between

4 and 5×10^{12} N m⁻¹. This force is thus comparable with, and possibly somewhat larger than, the ridge-push force for the large continental plateaus. Again, the actual stress magnitude in the upper lithosphere induced by this buoyancy force depends on lithosphere rheology and heat flow. Kuznir & Park (1987) compute stress amplification factors of as much as 8–11 for the middle crust for regions with surface heat flows of 95 mW m⁻².

Taking the stress amplification factor into account, it thus appears likely that buoyancy-related stresses may locally dominate the state of stress within the plate. Observed stress rotations (relative to regional, mid-plate orientations) in the vicinity of elevated regions can be used to place limits on the ratio of the magnitudes of regional versus local (buoyancy) stresses in the crust. Zoback (1991*a*) calculated that local buoyancy-derived extensional stresses in the upper lithosphere of the East African rift region must be roughly four times the magnitude of the regional stress differences in the plate to cause the roughly 60° rotation of the regional intraplate strike-slip stress régime with E–W $S_{H,max}$ to the observed normal faulting stress régime with a NNE trending $S_{H,max}$ in the vicinity of the East African rift. In many areas the superimposed effect of this buoyancy force may be more subtle. In the Colorado Plateau of the western United States, negative buoyancy forces associated with a relatively dense keel of upper mantle lithosphere have been suggested as the source of a 90° rotation of horizontal stresses between the extensional stress régimes of the Colorado Plateau and the surrounding Basin and Range (Zoback & Zoback, 1989).

As mentioned above, there are many normal faulting earthquakes in western Europe located distant from the Alpine belt and unrelated to any topographic effects due to that mountain chain. The stress orientation data in this region suggest that the origin of the mid-plate stress field in western Europe is largely related to compressional forces (ridge push and continental collision), thus dominantly strike-slip and thrust faulting earthquakes would be expected, as seen in mid-plate North America. Müller *et al.* (1991) conclude that local buoyancy forces related to mantle upwelling (e.g. beneath the Upper Rhine graben embayment and the Massif Central) may be responsible for the altered stress state.

(b) Influence of drag forces

As the lithospheric plates form the lid of a complex system of convection within the Earth's interior, forces resulting from relative motion the lithospheric plates and the upper mantle is another potential source of stress within the plates. There are several possible models of drag to choose from: resistive drag at the base of the plate opposing plate motions, so-called 'driving' drag in the direction of plate motion, drag due to 'counterflow' (mass flow from trenches back to ridges) or, drag due to mantle flow arising from density inhomogeneities throughout the mantle. As mentioned previously, resistive drag has generally been modelled as small and largely used to balance torque on the plates, the predicted $S_{H,max}$ orientations are antiparallel to the direction of absolute plate motion. The magnitude of the resistive drag forces are generally assumed proportional to the product of velocity, area, and a drag coefficient which may differ between cold thick continental lithosphere and thin, relatively warm oceanic lithosphere. Resistive drag would thus be expected to have greatest effect on fast moving, old continental plates such as Australia; however, evidence in central Australia for a correlation between absolute plate motion and $S_{H,max}$ orientation is weak (and could alternately be explained as a result

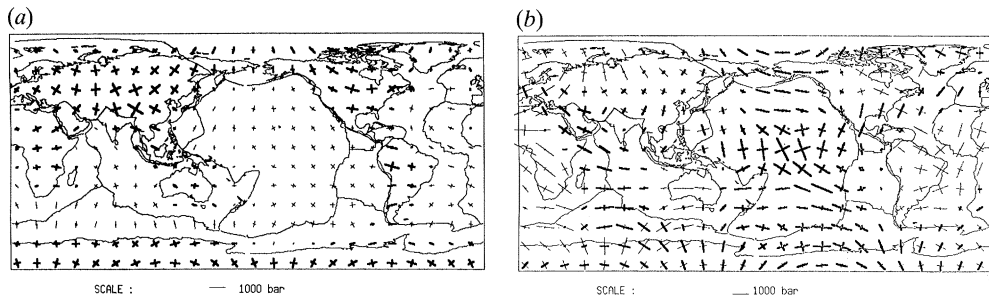


Figure 6. (a) Deviatoric stress patterns predicted from variations between oceanic and continental lithospheric density structure (expanded up to degree $l = 15$). The thick lines refer to extension, the thin ones to compression. (b) Superposition of 'reference' stress state (shown in (a)) and stresses arising from basal shear coupling due to mantle flow derived from a model driven by mass heterogeneities defined by seismic tomography and slab distribution. Figure from Bai *et al.* (1991) used with permission. (1000 bar = 10^8 Pa).

of ridge push and arc collision as explained above (see also Richardson 1991). Furthermore, zones of E–W compression on southeastern and southwestern coast of Australia would seem to rule this out.

Effects of counterflow drag are more difficult to evaluate. Counterflow calculations based on return of mass from the Aleutians to the mid-Atlantic ridge predict NW–SE directed flow beneath eastern North America (Chase 1979; Hager & O'Connell 1979). This is in clear disagreement with the well-constrained broad region of ENE trending $S_{H,max}$ directions in this region and implies that the counterflow must occur at a level too deep to influence stress states in the lithosphere (Zoback *et al.* 1986).

Models incorporating simple driving drag yield principal stress directions parallel and perpendicular to absolute plate motion and predict a stress gradient across the plate. Stress magnitudes due to drag are zero at the ridges and increase across the plate in the direction of absolute motion (Richardson *et al.* 1979; Richardson & Reding 1991). Inspection of the relative stress magnitude data shown in figures 3–5 show no clear evidence for systematic changes in the stress régime across plates except in North America, where normal faulting in the western United States is clearly a superimposed effect related to buoyancy forces derived from the warm upper mantle. Systematic drag-related stress gradients would not be expected for the Eurasian plate since its motion is so slow (barely resolvable in a hot-spot reference frame (Minster & Jordan 1978)). Relative stress magnitude data in the interior of South America are too sparse to evaluate.

For mid-plate North America (most of intraplate North America, excluding Alaska and all regions west of about the 1000 m contour shown on figures 1 and 2) Richardson & Reding (1991) calculated a 10-fold increase in stress magnitudes across the width of the plate due to drag. They point out that there is no evidence for such a variation; in mid-plate North America the horizontal stresses appear to decrease westward, not increase; deformation in the eastern United States is a mixture of thrust and strike-slip faulting whereas in the central U.S. it is dominantly strike-slip. Driving-drag models would predict an increase in thrust faulting in the central U.S.

A more complete evaluation of drag effects considers actual whole mantle flow patterns. Recent analysis of the geoid and of seismic tomography constrain broad-scale density inhomogeneities within the Earth's mantle. The resultant flow pattern

(including the effect of dense masses corresponding to oceanic slabs) has been calculated by Ricard & Vigny (1989). Recently, Bai *et al.* (1991) have computed the stresses in the lithosphere induced by the deep mantle flow pattern predicted by Ricard & Vigny. They superimposed the stresses calculated for this flow model on their proposed non-tectonic reference state of 50–100 MPa deviatoric extension in the continents and compression in the oceans computed from the contrast in density between oceanic and continental lithosphere structures (figure 6*a*). The resultant broad-scale lithospheric stress patterns for the superimposed effects of the mantle flow are shown in figure 6*b*.

One important effect of the stresses due to mantle flow is to put most continents into compression rather than extension (note that the mantle flow stresses include the broad-scale density effects of ridges and slabs). Bai *et al.* (1991) concluded that comparison of their predicted stress states with the observed stress data is premature because the coverage is spotty and so little information on absolute stress magnitudes is available. Furthermore, they state that significant variation in stress patterns are not resolvable for wavelengths less than 5000 km (a distance that roughly coincides to three of their computed grid points).

However, as described in §2 the available stress data define a number of broad areas (on the order of 5000 km on a side) of consistent stress orientations. Several prominent stress patterns predicted by their model poorly match the available stress observations even at this broad 5000 km wavelength. Specifically, Bai *et al.* predict NW–WNW $S_{H,max}$ directions in mid-plate North America which are inconsistent with the observed ENE compression; similarly, strong NE compression predicted for western Europe is in contrast with the observed NW compression. In addition, Bai *et al.* predict enormous deviatoric extensional stresses related to upwelling in the central Pacific, a region noted for its lack of intraplate seismicity. The predicted extensional stresses are greater than 100 MPa, nearly twice as large as predicted anywhere else on the globe, even the seismically active Indian Ocean. However, this prediction for the Pacific was based on an assumption of one-layer convection which also overpredicts the geoid high, it is likely that a two-layer convection model may be more appropriate (C. Froidevaux 1991, personal communication).

4. Conclusions

The mid-plate stress field in both the oceans and continents is largely compressional with one or both of the horizontal stresses is greater than the vertical stress. The orientation of the mid-plate stress field is consistent with plate-motion directions in many areas and seems to be influenced dominantly by plate-boundary forces (locally modulated by bouyancy forces). The geometry of the plate boundaries are extremely important in determining the broad-scale stress orientation patterns.

Regional variations in relative stress magnitude are defined based on direct stress measurements and the style of faulting. In most mid-plate areas a combination of thrust and strike–slip faulting régimes are observed. Most regions of normal faulting occur in areas of high elevation; the extensional stress régime in these areas can be attributed to superimposed bouyancy forces related to thickened crust and/or thin lithosphere and active mantle upwelling. To explain observed local stress rotations, the upper crustal stresses derived from these bouyancy forces must be several times the magnitude of the regional stress differences due to plate-boundary forces. In areas where normal faulting occurs in close proximity to thrust and strike–slip

faulting (such as in major mountain belts but also within western Europe) the $S_{H,max}$ orientations are consistent for all three stress régimes.

Evaluating drag is difficult with stress orientations alone. First-order patterns of stress orientation are well explained as the result of plate-boundary forces acting on plate geometry. However, in several cases the observed $S_{H,max}$ directions are subparallel to absolute velocity directions as well. Evidence for lateral stress gradients with an order of magnitude variation in stress values across large plates (predicted for models in which drag dominates (Richardson 1991; Richardson & Reding 1991)), is not observed in the relative stress magnitude data. Similarly, the broadest-scale patterns observed in the stress data do not match predictions of stress orientations related to whole mantle flow inferred from current generation seismic tomography models (Bai *et al.* 1991).

Thus the intraplate lithospheric stress fields appear to be dominated by plate-boundary and local bouyancy forces. However, since lithosphere plates are merely the uppermost part (boundary layer) of the Earth's convection system, the stress fields can always be linked ultimately to mantle convection.

The World Stress Map project is a collaborative effort of about 30 scientists worldwide who have actively compiled and contributed data: J. Adams, M. Assumpcao, S. Bell, E. A. Bergman, W. Bosworth, D. Denham, J. Ding, N. Gay, S. Gregersen, T. N. Gowd, G. Grunthal, A. Gvishiani, K. Jacob, P. Kropotkin, R. Klein, P. Knoll, M. Magee, J. L. Mercier, V. Mount, B. Müller, N. Pavoni, K. Rajendran, S. I. Sherman, O. Stephansson, D. Stromeyer, G. Suarez, M. Suter, A. Udias, Z. H. Xu, M. Zhizhin and M. D. Zoback.

References

- Assumpcao, M. 1991 The regional intraplate stress field in South America. *J. geophys. Res.* (In the press.)
- Artyushkov, E. V. 1973 Stresses in the lithosphere caused by crustal thickness inhomogeneities. *J. geophys. Res.* **78**, 7675–7708.
- Bai, W., Vigny, C., Ricard, Y. & Froidevaux, C. 1991 On the origin of deviatoric stresses in the lithosphere. *J. geophys. Res.* (In the press.)
- Chase, C. G. 1979 Asthenospheric counterflow: a kinematic model. *Geophys. Jl R. astr. Soc.* **56**, 1–18.
- Cloetingh, S. & Wortel, M. J. R. 1986 Stress in the Indo-Australian plate. *Tectonophysics*. **132**, 49–67.
- England, P. & Houseman, G. 1989 Extension during continental convergence, with application to the Tibetan. *J. geophys. Res.* **94**, 17561–17579.
- Fleitout, L. & Froidevaux, C. 1982 Tectonics and topography for a lithosphere containing density heterogeneities. *Tectonics* **1**, 21–56.
- Fleitout, L. & Froidevaux, C. 1983 Tectonic stresses in the lithosphere. *Tectonics* **2**, 315–324.
- Frank, F. C. 1972 *Plate tectonics, the analogy with glacier flow and isostasy. Flow and fracture of rocks*. Geophysics Monograph Ser. 16, pp. 285–292. AGU.
- Froidevaux, C. & Isacks, B. L. 1984 The mechanical state of stress of the Altiplano-Puna segment of the Andes. *Earth planet. Sci. Lett.* **71**, 305–314.
- Grunthal, G. & Stomeyer, D. 1991 The recent crustal stress field in central Europe – trajectories and finite-element modeling. *J. geophys. Res.* (In the press.)
- Hager, B. & O'Connell, R. J. 1979 Kinematic models of large-scale flow in the Earth's mantle. *J. geophys. Res.* **84**, 1031–1048.
- Henry, W. J., Mechie, J., Maguire, P. K. H., Khan, M. A., Prodehl, C., Keller, G. R. & Patel, J. 1990 A seismic investigation of the Kenya rift valley. *Geophys. J. Int.* **100**, 107–130.
- Isacks, B. L. 1988 Uplift of the central Andean plateau and bending of the Bolivian orocline. *J. geophys. Res.* **93**, 3211–3231.

- Jurdy, D. M. & Stefanick, M. 1991 Stress observations and driving forces models for the South American plate. *J. geophys. Res.* (In the press.)
- Kusznir, N. J. & Bott, M. H. P. 1977 Stress concentration in the upper lithosphere caused by underlying viscoelastic creep. *Tectonophys.* **43**, 247–256.
- Kusznir, N. J. & Park, R. G. 1984 Intraplate lithosphere deformation and the strength of the lithosphere. *Geophys. Jl R. astr. Soc.* **79**, 513–538.
- Kusznir, N. J. & Park, R. G. 1987 The extensional strength of the continental lithosphere: its dependence on geothermal gradient, and crustal composition and thickness. *Geol. Soc. Lond. Spec. Publ.* **28**, 35–52.
- Lister, C. R. B. 1975 Gravitational drive on oceanic plates caused by thermal contraction. *Nature, Lond.* **257**, 663–665.
- Meijer, P. Th. & Wortel, M. J. R. 1991 The dynamics of motion of the South American plate. *J. geophys. Res.* (In the press.)
- Minster, J. B. & Jordan, T. H. 1978 Present day plate motions. *J. geophys. Res.* **83**, 5331–5354.
- Molnar, P. & Tapponnier, P. 1975 Cenozoic tectonics of Asia: effects of a continental collision. *Science, Wash.* **189**, 419–426.
- Müller, B., Zoback, M. L., Fuchs, K., Mastin, L., Gregersen, S., Pavoni, N., Stephansson, O. & Ljunggren, C. 1991 Regional patterns of tectonic stress in Europe. *J. geophys. Res.* (In the press.)
- Parsons, B. & Richter, F. M. 1980 A relation between driving force and geoid anomaly associated with the mid-ocean ridges. *Earth planet. Sci. Lett.* **51**, 445–450.
- Ricard, J. & Vigny, C. 1989 Mantle dynamics with induced plate tectonics. *J. geophys. Res.* **94**, 17543–17559.
- Richardson, R. M. 1991 Ridge forces, absolute plate motions, and the intraplate stress field. *J. Geophys.* (In the press.)
- Richardson, R. M., Solomon, S. C. & Sleep, N. H. 1979 Tectonic stress in the plates. *Rev. Geophys. Space Phys.* **17**, 981–1019.
- Richardson, R. M. & Reding, L. M. 1991 North American plate dynamics. *J. geophys. Res.* (In the press.)
- Thompson, G. A. & Zoback, M. L. 1979 Regional geophysics of the Colorado Plateau. *Tectonophys.* **61**, 149–181.
- Wiens, D. & Stien, S. 1985 Implications of oceanic intraplate seismicity for plate stresses, driving forces, and rheology. *Tectonophys.* **116**, 143–162.
- Zoback, M. D. & Zoback, M. L. 1991 Tectonic stress field of North America and relative plate motions. In *Neotectonics of North America, decade of North American geology* (ed. B. Slemmons), Boulder, Colorado: Geological Society of America. (In the press.)
- Zoback, M. L. 1991a First and second order patterns of stress in the lithosphere: the World Stress Map project. *J. geophys. Res.* (In the press.)
- Zoback, M. L. 1991b Stress field constraints on intraplate seismicity in eastern North America. *J. geophys. Res.* (In the press.)
- Zoback, M. L., Nishenko, S. R., Richardson, R. M., Hasegawa, H. S. & Zoback, M. D. 1986 Mid-plate stress, deformation, and seismicity. In *The western North Atlantic region, Decade of North American geology* (ed. P. R. Vogt & B. E. Tucholke), vol. M. Boulder, Colorado: Geological Society of America.
- Zoback, M. L. & Zoback, M. D. 1989 Tectonic stress field of the continental United States. *Geol. Soc. Am. Mem.* **172**, 523–539.
- Zoback, M. L. *et al.* 1989 Global patterns of tectonic stress. *Nature, Lond.* **341**, 291–298.
- Zorin, Y. A. & Rogozhina, V. A. 1978 Mechanism of rifting and some features of the deep-seated structure of the Baikal rift zone. *Tectonophys.* **45**, 23–30.

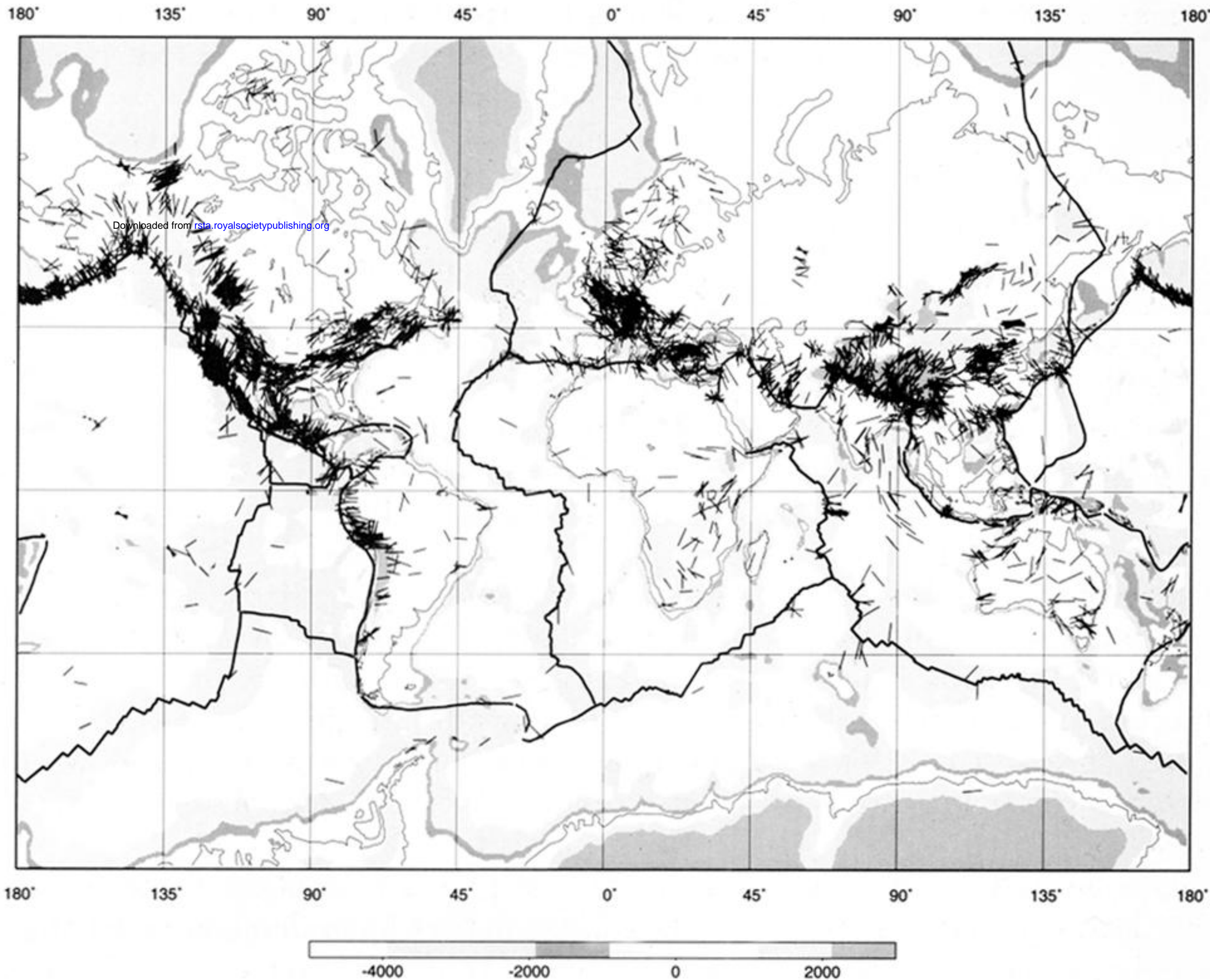
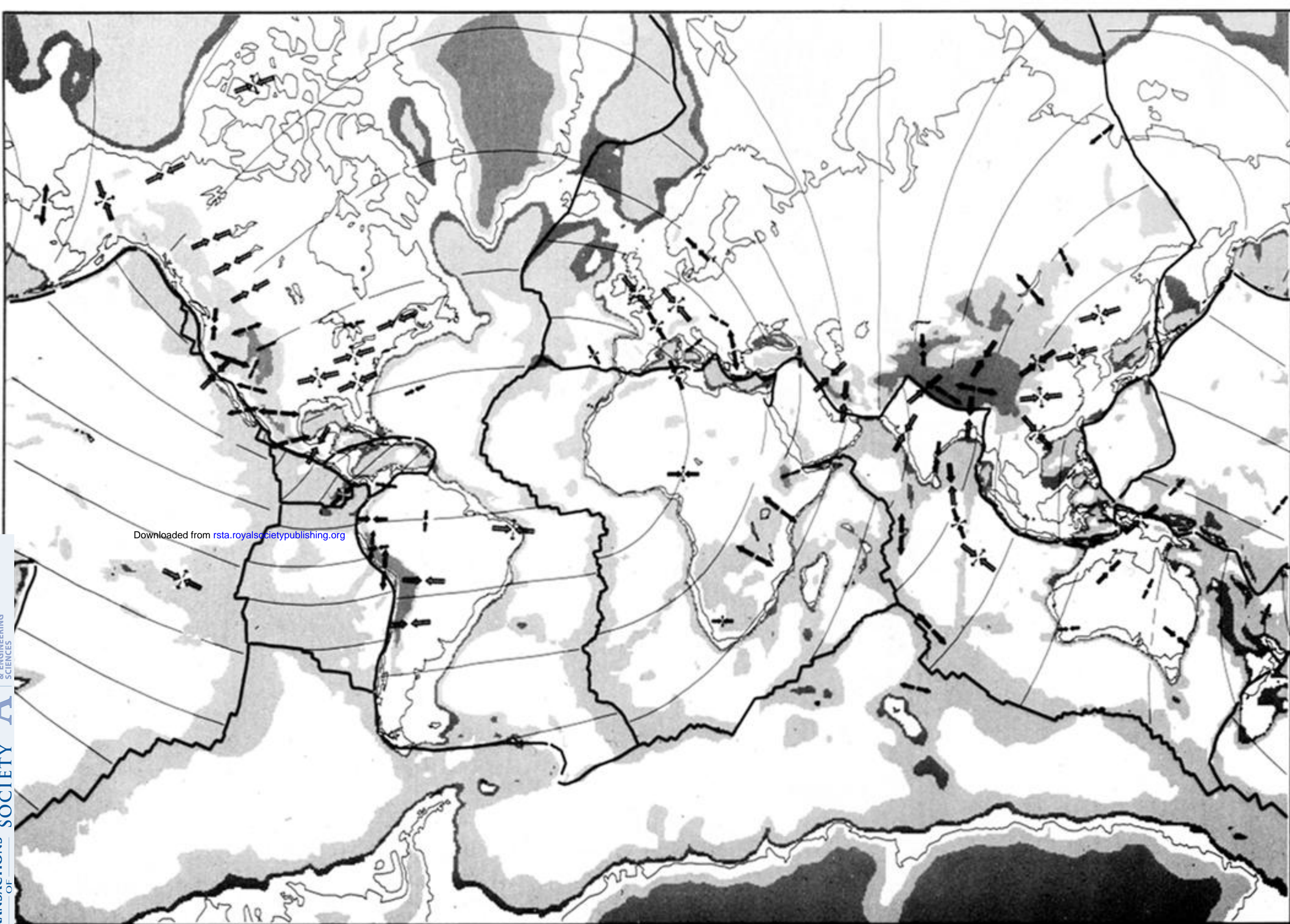


Figure 1. World Stress Map, Mercator projection. $S_{H,max}$ orientations are plotted, length of lines are proportional to quality.



Downloaded from rsta.royalsocietypublishing.org



Figure 2. Generalized stress map of the world. Large arrows indicate mean stress directions for dense clusters of data. Inward pointing arrows indicate $S_{H,\max}$ orientations for compressive stress regimes where $S_{H,\max}$ coincides with S_1 and one or both of the horizontal stresses exceeds the vertical stress. Outward pointing arrows show $S_{H,\min}$ orientations. Thick outward pointing arrows indicate regions of extensional stress régime where both horizontal stresses are less than the vertical stress. Thin outward pointing arrows plotted together with inward pointing arrows indicate a strike-slip faulting stress régime. Coverage is non-uniform due to the non-uniform data coverage (see figure 1. Light lines are absolute velocity trajectories from model AM1-2 of Minster & Jordan 1978).

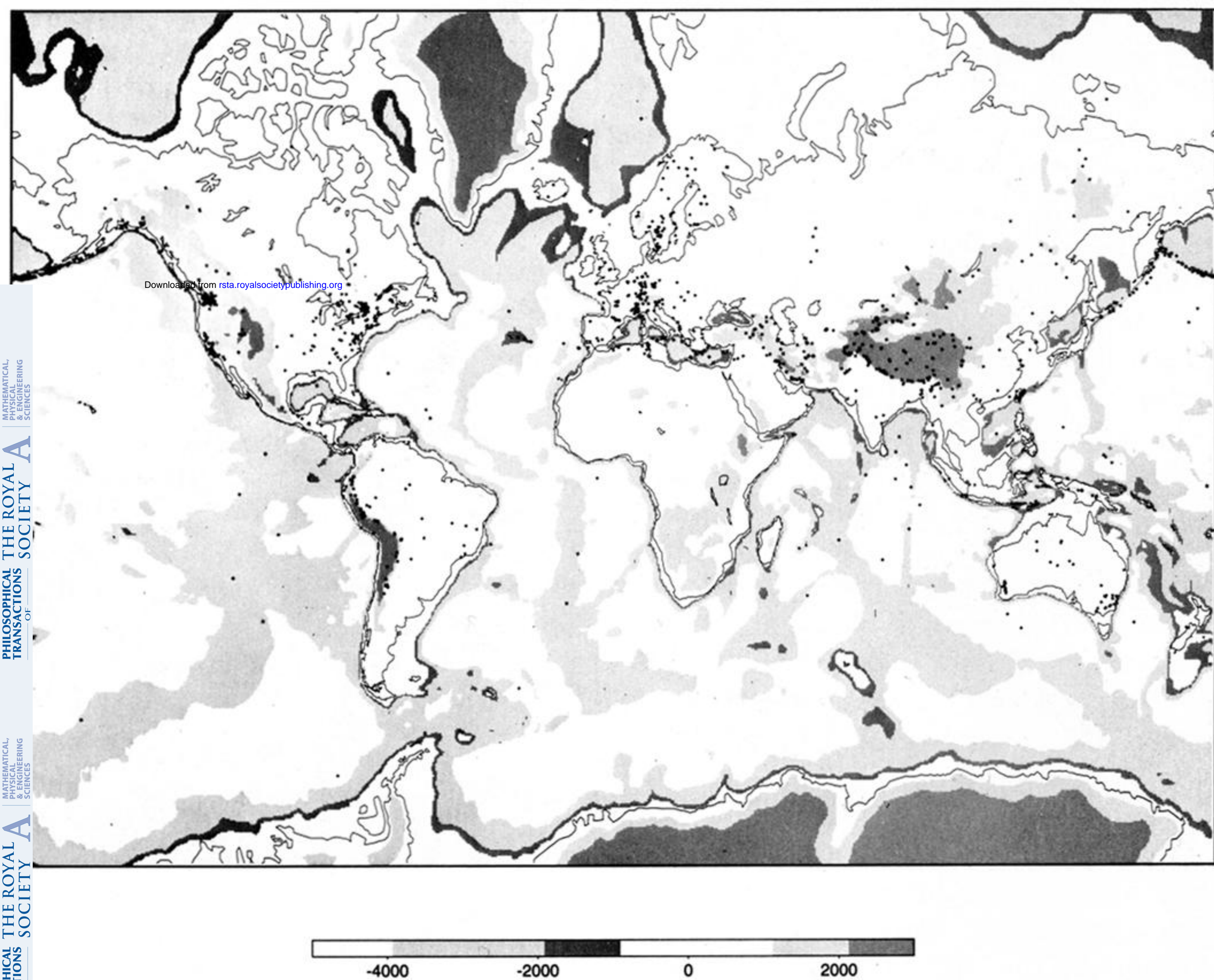


Figure 3. Location (by small crosses) of all data indicating a thrust faulting stress régime ($S_{H,max} > S_{H,min} > S_V$) in the WSM database.

Downloaded from rsta.royalsocietypublishing.org



Figure 4. Location (by small crosses) of all data indicating a strike-slip faulting stress régime ($S_{H,max} > S_V > S_{H,min}$) in the WSM database.

Downloaded from rsta.royalsocietypublishing.org



Figure 5. Location (by small crosses) of all data indicating a normal faulting stress régime ($S_V > S_{H,max} > S_{H,min}$) in the WSM database.